United States-Japan Bi-Lateral Seminar in Hydrology
Honolulu, January 1971

EFFECT OF AN ERROR IN DISCHARGE MEASUREMENTS ON THE DETECTION PROCESS IN RUNOFF SYSTEMS ANALYSIS

by Tsutomu Kishi
Professor, Department of Civil Engineering
Faculty of Engineering
Hokkaido University
Sapporo, Japan

Synopsis

A river basin acts as a low pass filter in the prediction process and becomes an amplifier for high frequency bands in the detection process.

First, theoretical considerations are made about the detection process for a basin of the cascade-connected linear reservoirs. Theoretically speaking, the possibility of obtaining the time function of input depends on the functional form of the output and on the order of the system or the number of linear reservoirs.

An approximate method of calculation by which the Fourier inverse transform of the detected input function is always integrable is presented. Results of calculations using field data are described as illustrative examples. The author points out that the precision of the detected values of the input decreases markedly if even a small error is contained in the measurements of the output.

Then, the author investigates the relation of turbulence characteristics of natural streams to the error in velocity measurements which must be a signigicant factor affecting the total error in discharge measurements. It is pointed out that the error in velocity measurements can be decreased appreciably if the observational period at a point is prolonged by a small fraction of time.

1. Introduction

The use of the transform methods in runoff systems analysis has been mainly made for the processes of identification and prediction and few attempts have been made for the detection process. However, it becomes often necessary both in practical designs and in research to detect the precipitation, which happens to be missed, from the runoff records and a given system function. To this end, it is important to investigate a methodology of the detection process.

In the prediction process a river basin is a low pass filter. To the contrary, it acts as an amplifier for high frequency bands in the detection process. The rate of amplification would depend on the functional form of output and on the frequency characteristics of the basin system. Since the shorter the duration of a pulse in the output the wider the Fourier spectrum becomes, an error of short duration in discharge measurements would result in the detection process. This fact brings forth various problems which should be studied before the detection process in runoff systems analysis comes into operation.

The total error in discharge measurements in natural streams comes from various origins. The turbulence in streams must be a significant factor among them. The relationship between the error of the mean velocity observed at a point and the period of observation will be derived from the power spectra of velocity fluctuations. This kind of research is an essential basis in obtaining the precise records of stream discharge which are especially necessary in the calculation of the detection process.

2. Theoretical considerations

Let us consider a basin system which consists of a linear reservoir cascade with n elements. The systems frequency function $G(\omega)$ is given by

$$G(\omega) = \left(\frac{\lambda}{\lambda+j\omega}\right)^n \tag{1}$$

where ω : angular frequency
λ : storage factor (reciprocal of storage constant)
j : imaginary unit
n : number of linear reservoirs

In the frequency domain, the Fourier transform of input $I(\omega)$ is related to the output $Q(\omega)$ with

$$I(\omega) = Q(\omega)/G(\omega) \tag{2}$$

Since the time function of input $I(t)$ must be a causal function, the absolute value of $I(\omega)$ must be square-integrable:

$$\int_{-\infty}^{\infty} |I(\omega)|^2 \, d\omega < \infty \tag{3}$$

Thus, the function $Q(\omega)$ must be at least such that

$$Q(\omega) = o\{G(\omega)\} \qquad (\omega \to +\infty) \tag{4}$$

where o = Landau notation, which means
$Q(\omega)/G(\omega) \to o$ for $\omega \to +\infty$

It is not necessarily true that an arbitrary output function always satisfies condition (4). This will be shown by the following illustrative examples.

Suppose that a triangular pulse shown in Fig. 1 is given as the output at time $t = t_o$. The Fourier transform pair is

$$Q_B(t-t_o) \longleftrightarrow \frac{4\sin^2(\omega B/2)}{B\omega^2} e^{-j\omega t_o} \tag{5}$$

Thus, the time functions of input for the single reservoir system (n = 1) and two cascaded reservoirs system (n = 2) are given by equations (6) and (7), respectively.

single reservoir system

$$I(t) = \frac{2}{\pi}\int_o^{\infty} \frac{4\sin^2(\omega B/2)}{\lambda B\omega^2} (\lambda\cos\omega t_o + \omega\sin\omega t_o)\cos\omega t \, d\omega \qquad t > 0 \tag{6}$$

two cascaded reservoirs system

$$I(t) = \frac{2}{\pi}\int_o^{\infty} \frac{4\sin^2(\omega B/2)}{\lambda^2 B\omega^2} [(\lambda^2-\omega^2)\cos\omega t_o + 2\lambda\omega\sin\omega t_o]\cos\omega t \, d\omega \qquad t > 0 \tag{7}$$

Equation (6) is integrable because the integrand on the right hand side satisfies condition (4). In Fig. 2 results of numerical calculation for two cases described in the following table are shown. For this problem Laplace transform is more convenient to investigate the functional form of I(t). Indeed, input function I(s) is given by

$$I(s) = Q(s) + \frac{1}{B\lambda} \cdot \frac{1}{s} \left[e^{-(t_o - B)s/2} - e^{-(t_o + B)s/2} \right]^2 \qquad (8)$$

Table: Conditions for numerical calculation

	Case 1 (Fig. 2a)	Case 2 (Fig. 2b)
$\lambda(hr^{-1})$	0.1	0.1
B(hr)	1.0	1.0
t_o(hr)	10.0	20.0
$\Delta\omega$(radian/hr)	0.05	0.05
ω_{max}(radian/hr)	150	150
$I(\omega_{max})/I(\omega)_{max}$	0.009	0.015

ω_{max} means the highest value of frequency over which $I(\omega)$ is truncated. $I(\omega)_{max}$ is the maximum value of $I(\omega)$

Equation (8) shows that I(t) is the sum of the output Q(t) and two successive rectangular pulses with different sign (positive and negative). The height of rectanglular pulses is amplified by the factor $1/B\lambda$.

Since the inverse Fourier transform given by equation (6) is calculated at discontinuities, Gibb's phenomenon[1] appeares in the results of the numerical calculation.

Fig. 2b shows the effect of truncation error.

Contrary to equation (6), however, equation (7) is not integrable as will be easily recongnized.

For the next example we shall consider the output to be a rectangular pulse as shown in Fig. 3. The time functions I(t) are:

single reservoir system

$$I(t) = \frac{2}{\pi} \int_o^\infty \frac{2\sin\omega B}{\lambda\omega} (\lambda\cos\omega t_o + \omega\sin\omega t_o)\cos\omega t d\omega \qquad (9)$$

$t > 0$

two cascaded reservoirs system

$$I(t) = \frac{2}{\pi} \int_o^\infty \frac{2\sin\omega B}{\lambda^2\omega^2} [(\lambda^2 - \omega^2)\cos\omega t_o + 2\lambda\omega\sin\omega t_o]\cos\omega t d\omega \qquad (10)$$

$t > 0$

It is easily seen that both solutions are meaningless unless the concept of distributions is introduced. For instance, $I(\omega)$ for equation (9) is

---

1) Papoulis, A., "The Fourier Integral and its Application", McGraw-Hill, 1962, p. 30

$$I(\omega) = \frac{2\sin\omega B}{\omega} e^{-j\omega t_o} + \frac{j}{\lambda} 2\sin\omega B e^{-j\omega t_o} \tag{11}$$

Obviously, the first term of the right hand side is $Q(\omega)e^{-j\omega t_o}$. The transform pair for the second term is obtained by considering the symmetrical character[2)]

$$\frac{1}{\lambda}\left[\delta\{t-(t_o-B)\} - \delta\{t-(t_o+B)\}\right] \longleftrightarrow \frac{j}{\lambda} 2\sin\omega B e^{-j\omega t_o} \tag{12}$$

Consequently, the time function $I(t)$ is

$$I(t) = Q(t-t_o) + \frac{1}{\lambda}\left[\delta\{t-(t_o-B)\} - \delta\{t-(t_o+B)\}\right] \tag{13}$$

The function $I(t)$ given by equation (13) is shown in Fig. 3.

As stated above the evaluation of the inverse Fourier transform is not always easy even under relatively simple conditions. Consequently, in the detection process for actual basin systems under more complicated circumstances it is necessary to develop a method of numerical calculation especially suitable for computer calculations.

3. Presentation of a method of numerical calculation

A necessary and sufficient condition for a square-integrable function $A(\omega) \geq 0$ to be the Fourier spectrum of a causal function is the Paley-Wiener condition[3)]

$$\int_{-\infty}^{\infty} \frac{|\ln A(\omega)|}{1+\omega^2} d\omega < \infty \tag{14}$$

Consequently, the absolute value of $I(\omega)$ detected must satisfy condition (14).

A method of numerical calculation which satisfies the Paley-Wiener condition is as follows:

Approximating the output $Q(t)$ by a polygon as shown in Fig. 4a, and differentiating twice,

$$\begin{aligned} Q(\omega) &= -\frac{1}{\omega^2}\left\{\frac{k_1}{(t_2-t_1)} e^{-j\omega t_1} + \frac{k_2}{(t_3-t_2)} e^{-j\omega t_2} + \cdots\cdots \right. \\ &\quad \left. + \frac{k_n}{(t_n-t_{n-1})} e^{-j\omega t_n}\right\} \\ &= -\frac{1}{\omega^2}\{Q_R(\omega) + jQ_X(\omega)\} \end{aligned} \tag{15}$$

where $Q_R(\omega)$, $Q_X(\omega)$: real and imaginary part of $-Q(\omega)\cdot\omega^2$

---

2) c.f. 1), p. 14
3) c.f. 1), pp. 215-217

Approximating the impulse response $G(t)$ by step functions as shown in Fig. 4b and differentiating once,

$$G(\omega) = \frac{1}{j\omega}\left[k_1 e^{-j\omega t_1} + k_2 e^{-j\omega t_2} + \cdots + k_n e^{-j\omega t_n}\right] \tag{16}$$

$$= -\frac{1}{\omega}\left\{-G_X(\omega) + jG_R(\omega)\right\}$$

where $G_R(\omega)$, $G_X(\omega)$: real and imaginary part of $-G(\omega)\cdot\omega$

Consequently,

$$I(\omega) = \frac{1}{\omega}\cdot\frac{1}{G_R^2+G_X^2}\left\{(-Q_R G_X+Q_X G_R) - j(Q_R G_R+Q_X G_X)\right\} \tag{17}$$

As will be seen in equations (15) and (16)

$$\left|\begin{matrix}Q_R\\Q_X\end{matrix}\right| \le \left|\frac{k_1}{t_2-t_1}\right| + \left|\frac{k_2}{t_3-t_2}\right| + \cdots \left|\frac{k_n}{t_n-t_{n-1}}\right| \tag{18}$$

($\equiv$M, a positive finite value)

$$\left|\begin{matrix}G_R\\G_X\end{matrix}\right| \le |k_1| + |k_2| + \cdots |k_n| \tag{19}$$

($\equiv$N, a positive finite value)

Therefore

$$|\omega I(\omega)| \le \frac{2MN}{G_R^2+G_X^2} \qquad (\equiv k, \text{ a positive finite value}) \tag{20}$$

Thus

$$A(\omega) = |I(\omega)| \le |k/\omega| \tag{21}$$

Consequently,

$$\lim_{\omega\to\pm\infty}\frac{|\ln A(\omega)|}{1+\omega^2} = \lim_{\omega\to\pm\infty}\frac{|\ln\omega|}{1+\omega^2} = 0 \tag{22}$$

The Paley-Wiener condition is, thus, satisfied.

Though the Paley-Wiener condition does not immediately mean that $I(\omega)$ has a causal inverse, it is permissible to regard the inverse transform of $I(\omega)$ as an approximation of a causal function $I(t)$ because an actual runoff system in which $I(t)$ must be a causal function is being considered.

Numerical examples for the Teshio river basin are shown in Figs. 5 and 6. A point to be worthy of note is the fact that much attention should be paid to the high frequency domains of output and basin system function, since the

function $I(t)$, in many cases, spreads up to a considerably high frequency domain because of its relatively short duration.

In Fig. 5 the values of $G(\omega)$ calculated from two flood records at the Pifuka gaging station[4] are compared. It is found that curves of $G(\omega)$ are nearly identical for $\omega < 0.6$ and the system frequency function for this basin can be assigned, if necessary. However, for $\omega > 0.6$ it is difficult to prescribe a precise value of $G(\omega)$, since the small fluctuations on the $G(\omega)$ curve seem to be rather random. These fluctuations would probably be due to the observational errors contained in $I(t)$ and $Q(t)$. The absolute value of $G(\omega)$ for $\omega > 0.6$ is damped so small that the effect of errors in observations would become evident.

A typical example is found in the $G(\omega)$ curve for flood No. 1 shown in Fig. 5. A distinct fluctuation in the $G(\omega)$ curve is observed for ω between 1.0 and 1.3. In this range of ω, the absolute value of $I(\omega)$ is particulary small, so that a small change in the value of $Q(\omega)$ has an appreciable effect on the value of $G(\omega)$. Indeed, the order of magnitude of $|Q(\omega)|$ in this range of ω is 10^{-1} mm. On the one hand, the total rainfall for flood No. 1 is 23.7 mm. Consequently, if there is an error pulse in the discharge measurement corresponding to approximately 0.5 % of the total effective rainfall, its Fourier spectrum would have the same order of magnitude as $|Q(\omega)|$. Thus, the value of $G(\omega)$ is very changeable.

In most cases the systems frequency function $G(\omega)$ is damped faster than $Q(\omega)$ and $I(\omega)$. And, as stated above, it is usually difficult to prescribe the precise value of $G(\omega)$ for $\omega > \omega_c$, where ω_c is a truncation frequency. For this reason, a function $P(t)$ which is an approximate estimate of $I(t)$ is plotted in Fig. 6.

The function $P(t)$ is obtained by the following way[5]. If $I(\omega)$ is truncated above a constant ω_c and the resulting function is designated by $P(\omega)$

$$P(\omega) = I(\omega)p\omega c(\omega) = 0 \qquad |\omega| > \omega_c \tag{23}$$

where $p\omega c(\omega)$: truncation filter

The inverse transform $P(t)$ can be found by expanding $P(\omega)$ into a Fourier series in the $(-\omega_c, \omega_c)$ interval:

$$P(\omega) = \sum_{n=-\infty}^{\infty} A_n e^{-jn\pi\omega/\omega_c} \tag{24}$$

where

$$A_n = \frac{1}{2\omega_c} \int_{-\omega_c}^{\omega_c} P(\omega) e^{jn\pi\omega/\omega_c} \, d\omega \tag{25}$$

$P(t)$ is, then, given by

$$P(t) = \frac{\omega_c}{\pi} \sum_{n=-\infty}^{\infty} An \, \frac{\sin(\omega_c t - n\pi)}{\omega_c t - n\pi} \tag{26}$$

---

4) Yamaoka, I., Fujita, M, Evaluation of Simulation Models For River Runoff Through Niquist Plots, Proc, Vol. 1, 13th I.A.H.R., Kyoto, 1969, pp. 171-180.
5) c.f. 1) p. 59

From the above we have

$$P\left(\frac{n\pi}{\omega_c}\right) = \frac{\omega_c A_n}{\pi} \tag{27}$$

The function $P(t)$ is related to $I(t)$ by

$$P(t) = \int_{-\infty}^{\infty} I(t) \frac{\sin\omega_c(t-\tau)}{\pi(t-\tau)} d\tau \tag{28}$$

For sufficiently large ω_c we have

$$I(t) \simeq P(t) \tag{29}$$

The values of rainfall detected by the above method are shown in Figs. 6(a) and (b) by the dotted line. Owing to the truncation error the total rainfall detected is not identical with the total rainfall. Then, the detected value was corrected to make the total rainfall detected be equal to the total rainfall[6]. The results are shown in Figs. 6(a) and (b) by the solid line.

4. Considerations to the precision of velocity measurements in natural streams[7]

4.1 Variance-duration curve for the mean velocity

The precision of velocity measurements in natural streams depends on the duration of the observation. The mean velocity U observed at any point during a time T_* is considered as a stochastic quantity the distribution of which is a function of T_*. The relation between the variance of U and the observational period T_* is called as the variance-duration curve and given by

$$C(T_*) = \frac{2C(0)}{T_*^2} \int_0^{T_*} (T_*-\tau)R_E(\tau)d\tau \tag{30}$$

where $C(T_*)$: variance of mean velocity observed during T_*
$C(0)$: variance of mean velocity for $T_* = 0$, that is the square of turbulence intensity of the flow
$R_E(\tau)$: auto-correlation function of the velocity fluctuation Subscript E designates the Eulerian correlations

For $T_* \gg T_E$, where T_E is the Eulerian integral time scale defined by $T_E = \int_0^{\infty} R_E(\tau)d\tau$, equation (30) gives

$$\frac{C(T_*)}{C(0)} \simeq 2\frac{T_E}{T_*} \quad \left(= 2\frac{L_x}{UT_*} \right) \tag{31}$$

---

6) Total rainfall is obtained by (Total runoff height/Runoff coefficient). If the runoff coefficient is a function of total rainfall, it is sometimes the case, all the calculations should be done with the effective rainfall.

7) Kishi, T., Mori, A., and Hirayama, K., Study on the Mechanics of Turbulence in Relation to the Analysis of the Accuracy of Velocity Measurements in natural Rivers, Rept. Faculty of Eng., Hokkaido Univ., July, 1970 (in Japanese)

where L_x is the macro scale of turbulence defined by $L_x = UT_E$.

It is noticed from equation (31) that no other length scale relating to the geometry of the river section is contained in $C(T_*)$ when T_E or L_x/U is considered as the unit of time scale. Equation (31) is an important relation in the consideration of the generalized expressions for turbulence characteristics in natural streams.

As is well known, the following relations hold between the auto-correlation function and the power spectrum:

$$R_E(\tau) = \frac{1}{u^2}\int_0^\infty E(f)\cos 2\pi f\tau \, df \tag{32}$$

$$E(f) = 4u^2\int_0^\infty R_E(\tau)\cos 2\pi f\tau \, d\tau \tag{33}$$

where

$E(f)$: power spectral density of turbulence
f : frequency
u^2 : energy of turbulence, that is square of turbulence intensity

Since $E(0) = 4u^2T_E$, the relation of $E(f)/u^2T_E$ v.s. T_Ef is the normalized power spectrum of turbulence. When the normalized power spectrum is approximated by an exponential function its functional form should be[8)]

$$\frac{E(f)}{u^2T_E} = 4\exp\{-4T_Ef\} \tag{34}$$

Substituting equation (34) into equation (30) thru equation (32) and integrating

$$\frac{C(T_*)}{C(0)} = 2\frac{\tan^{-1}\omega}{\omega} - \frac{\ln(\omega^2+1)}{\omega^2} \tag{35}$$

where

$$\omega = \frac{\pi}{2}\cdot\frac{T_*}{T_E}$$

4.2 Comparison with the field measurements

Velocity measurements were performed in three rivers in Hokkaido --- the Ishikari river, the Chitose river and the Shin river in 1968 and 1969. The Ishikari river at Hashimoto-cho station which is more than 100 m wide and around 3 m deep was selected as an example of large scale channel. The Chitose river at A and B stations which is around 30 m wide and 1 m deep is the example of a moderate channel. The Shin river which is 10 m wide and 0.5 m deep is an example of a small scale channel.

For the normalized power spectra, a comparison of equation (34), shown as a dasned curve, with field measurements is shown in Fig. 7. In spite of a wide range of variety in the geometry of gaging stations equation (34) agrees favorably with the field measurements.

---

8) c.f. 7)

The theoretical variance-duration curve of $C(T_*)/C(0)$ versus T_*/T_E given in equation (35) is compared with field measurements in Fig. 8. The solid line in the figure shows equation (35) and the dotted line shows the asymptotic relation (31). It is seen that equation (35) agrees favorably with the field measurements and equation (31) is also applicable for $T_*/T_E > 15$.

In the discussions so far, the magnitude of the integral time scale T_E or the macro scale of turbulence L_x has not yet been mentioned. These quantities presumably show a complicated dependence on the depth of water. The scale of the vortices in an open channel flow will mainly be controlled by the water depth if the water depth is small. However, if the water depth is large the scale of vortices will be related to the width of the flow as well.

The data of measurements shown in Figs. 7 and 8 were all obtained during a low water period. Therefore, the water depth would be the controlling length of the vortices. Fig. 9 shows the variation of L_x/H , where H is the water depth, with Z/H , where Z is the height above the bottom. Rough values of L_x/H range from 3 to 4, though they increases from the bottom towards the surface. Thus, the rough estimation of T_E is $(3 \sim 4) \cdot H/U$.

4.3 Importance of increasing the precision in velocity measurements

In the previous chapter, the author pointed out that a specially high precision in the output data is necessary in the operation of the detection process. The total error contained in the output measurements comes from various origins. However, there is no doubt that the error in velocity measurements is one of an important factor among them. Especially, for high water the discharge measurements must be of high reliability, since the number of data from which the stage-discharge relationship is derived is usually limited.

With this respect, the author would like to call attention to a blind spot in the hydrometric practive. For instance, in the "Guide to Hydrometeorological Practice", edited by W.M.O in 1965, only a space of nine words which follow is devoted to the observational period in velocity measurements.

"The velocity is observed . . . . . by conuting the number of revolutions of the rotor during a period of not less than 60 seconds.

The author would like to propose the following standard for the observational period in velocity measurements:

$$T_* \geq 5T_E$$

According to the above standard the standard deviation of the observed mean velocity at a point will be decreased to 50 % of the turbulence intensity, that is r.m.s of the velocity fluctuation of the flow. In the present practive of velocity measurements, the observational period for flood runoff would be at longest

$$T_* \simeq T_E$$

If the above evaluation is not wrong, the standard deviation of the observed mean velocity is as great as 90 % of the turbulence intensity. If we wish to decrease the value of standard deviation to 50 % of the turbulence intensity by increasing the number of observation points, the observation points have to be increased more than three times the number of the original points.

As will be recongnized, it is important and useful to enact a standard for the practice of velocity measurements by which the required precision is attained.

5. Conclusion

In this paper, mathematical considerations were made for the detection process in runoff systems analysis. The value of the Fourier transform function of the input to be detected should be calculated in the frequency domain with precision up to a high frequency region of ω in order to detect the detailed form of the input function. However, the above is not always easy because the Fourier spectra of the output and the systems frequency function decay to small value in the relatively low frequency region of ω and, consequently, the value of the Fourier spectra are disturbed by various noises in the high frequency domain. The fact that no methods such as the cross-correlation method in the identification process are found to eliminate the effects of noise would be a difficulty in the detection process. This fact will be understood through the examples given in chapter 3. In this meaning, a high precision in the discharge measurements is especially necessary in the detection process and a discussion concerning the hydrometric practice was presented.

Acknowledgement

The author wishes to thank to Mr. Mutsuhiro Fujita, Assistant Professor, Department of Civil Engineering, Hokkaido University, for his cooporation in this study. He performed the numerical calculations shown in Chapt. 3. And the author is also grateful to Professor Isao Yamaoka, Department of Civel Engineering, Hokkaido University, who kindly offered me the runoff data for the Teshio river at Pifuka.

List of Symbols

$A(\omega)$ = square-integrable function;
B = duration of pulse;
$C(T_*)$ = variance of mean velocity observed during T_*;
$E(f)$ = power spectral density of turbulence;
f = frequency;
$G(\omega)$ = systems frequency function;
$G_R(\omega)$, $G_X(\omega)$ = real and imaginary parts of $-G(\omega)\cdot\omega$;
H = water depth;
$I(\omega)$ = Fourier transform of input;
$I(\omega)_{max}$ = maximum value of $I(\omega)$;
j = imaginary unit;
L_x = macro scale of turbulence;
n = number of linear reservoirs;
$P(t)$ = approximate estimate of $I(t)$;
$p\omega_c(\omega)$ = truncation filter;
$Q(\omega)$ = Fourier transform of output;
$Q_R(\omega)$, $Q_X(\omega)$ = real and imaginary parts of $-Q(\omega)\omega^2$;
$R_E(\tau)$ = auto-correlation function of velocity fluctuation;
s = parameter of Laplace transform;
t = time;
T_* = duration of observation;
T_E = Eulerian integral time scale;
U = mean velocity;
ω = angular velocity;
ω_{max} = truncation frequency;
λ = storage factor (reciprocal of storage constant); and
δ = Dirac's delta function.

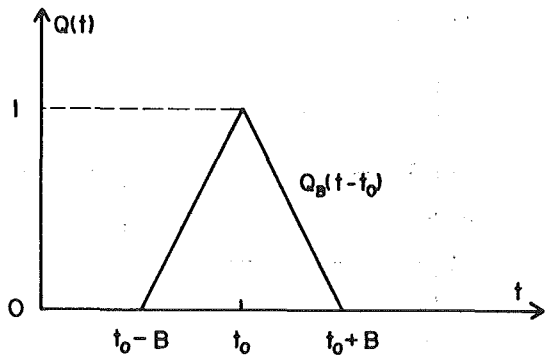

Fig. 1 Triangular pulse in output.

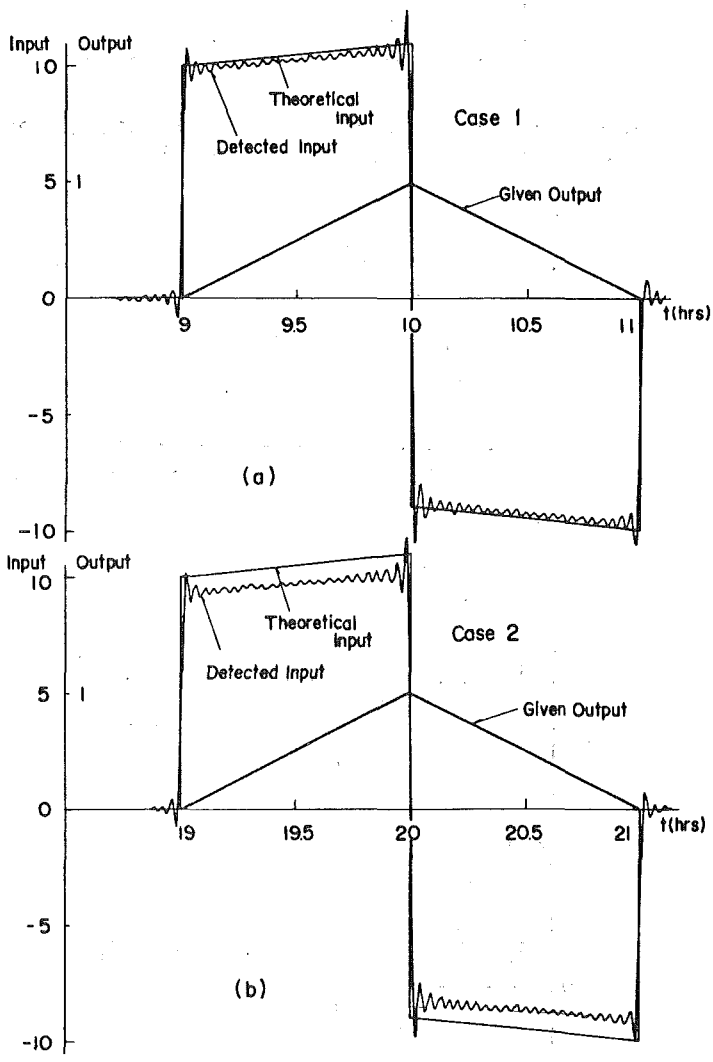

Fig. 2 Comparison of the detected input with theory. (Output of triangular pulse; lst order system)

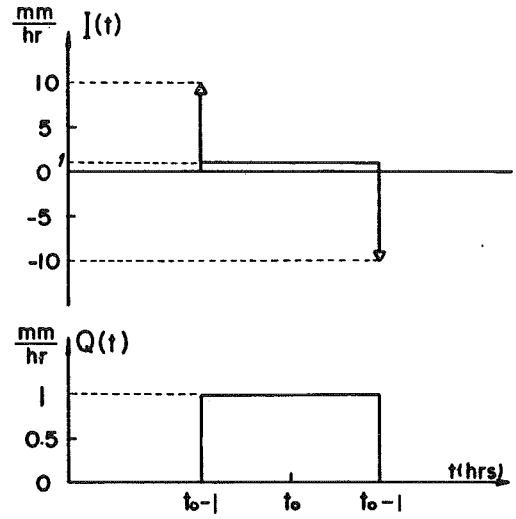

Fig. 3 Rectangular pulse in output and corresponding input (λ=0.1 hr^{-1}, B=1 hr in Eq.(13)).

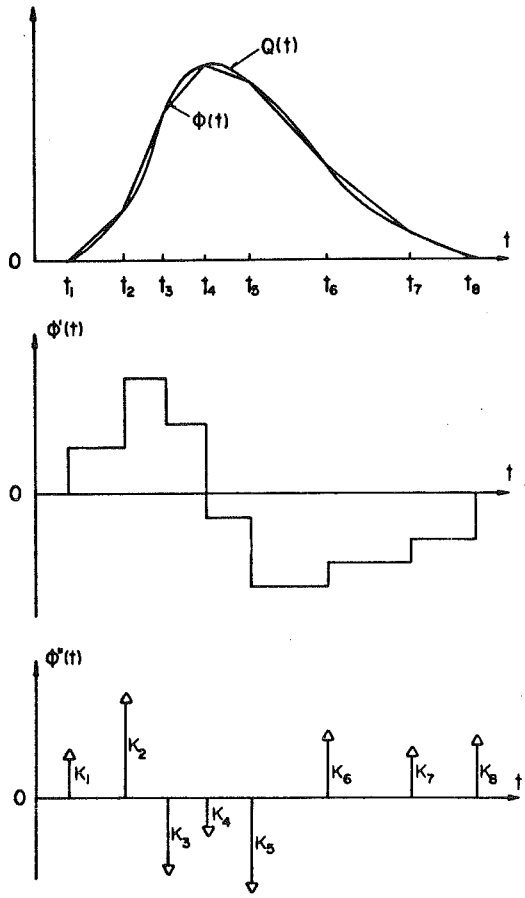

Fig. 4a. Polygonal approximation of Q(t).

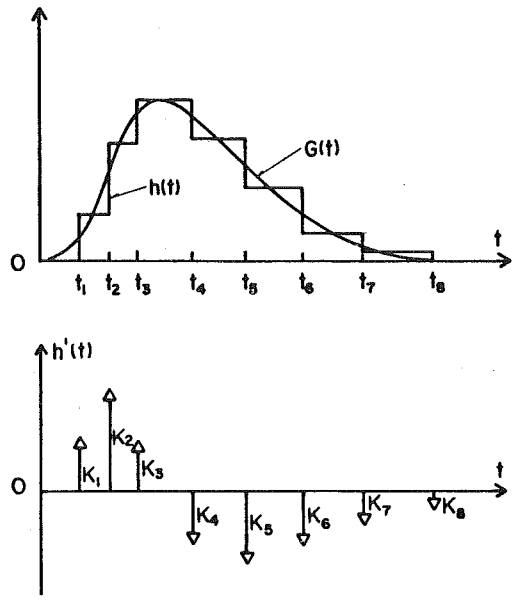

Fig. 4b Step approximation of G(t).

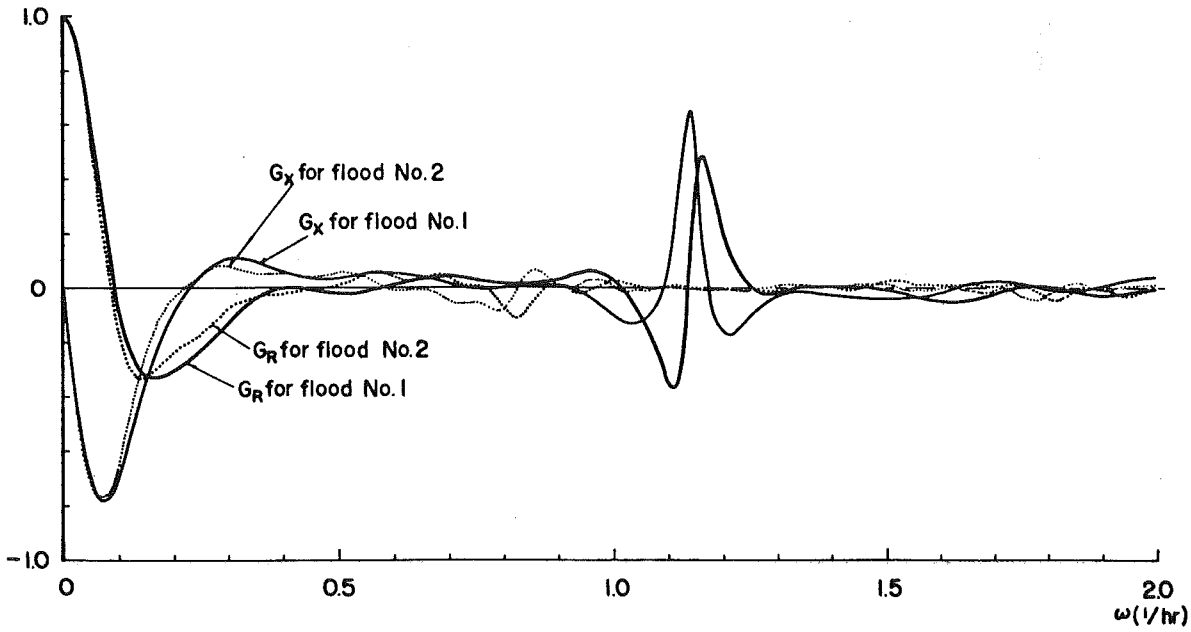

Fig. 5 System frequency function for the Teshio River at Pifuka.

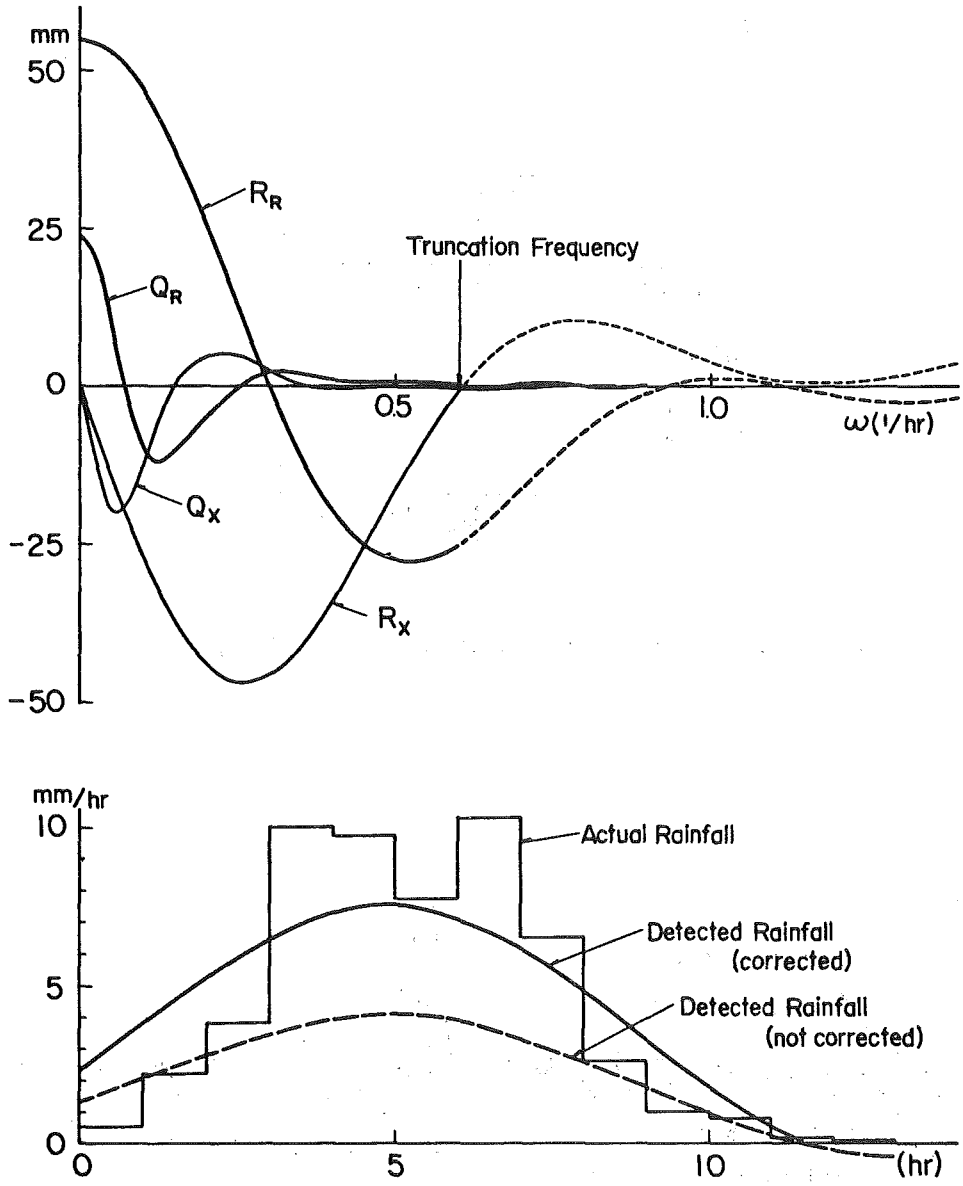

Fig. 6a Detection process for the Teshio river basin at Pifuka (flood No. 1)

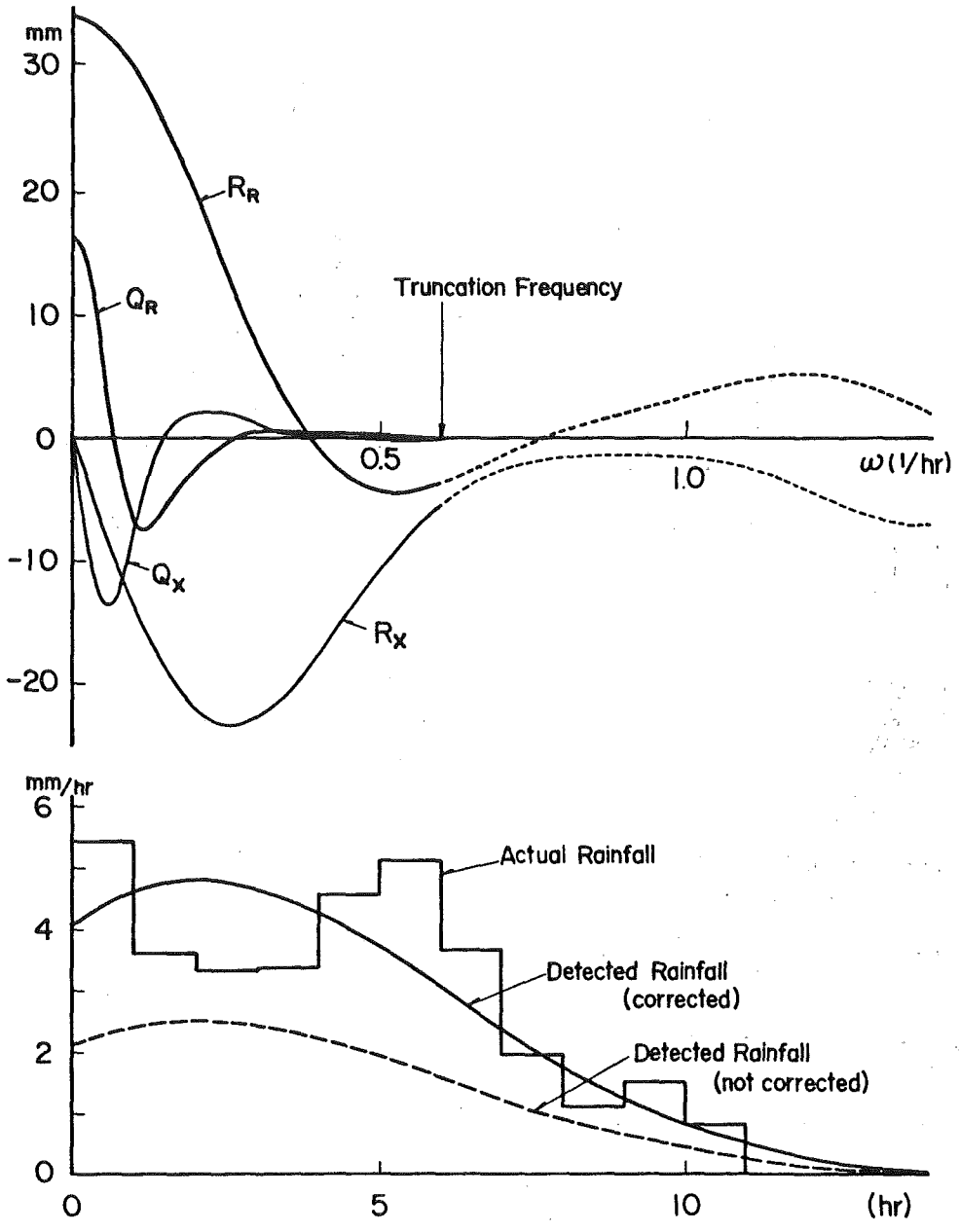

Fig. 6b Detection process for the Teshio river basin at Pifuka (flood No. 2).

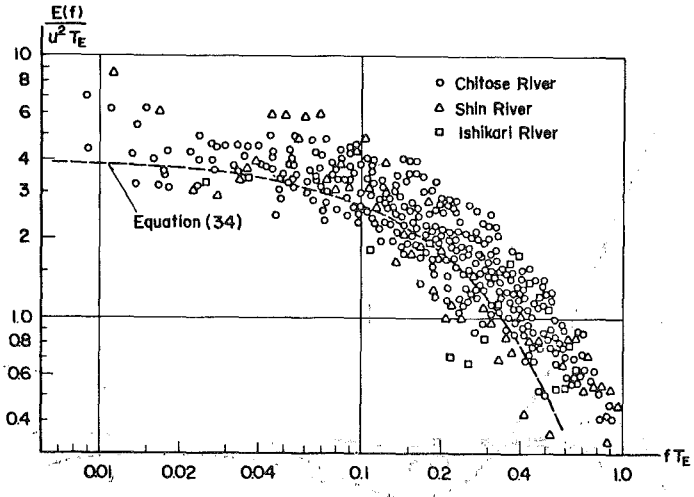

Fig. 7 Spectra of turbulence in natural streams.

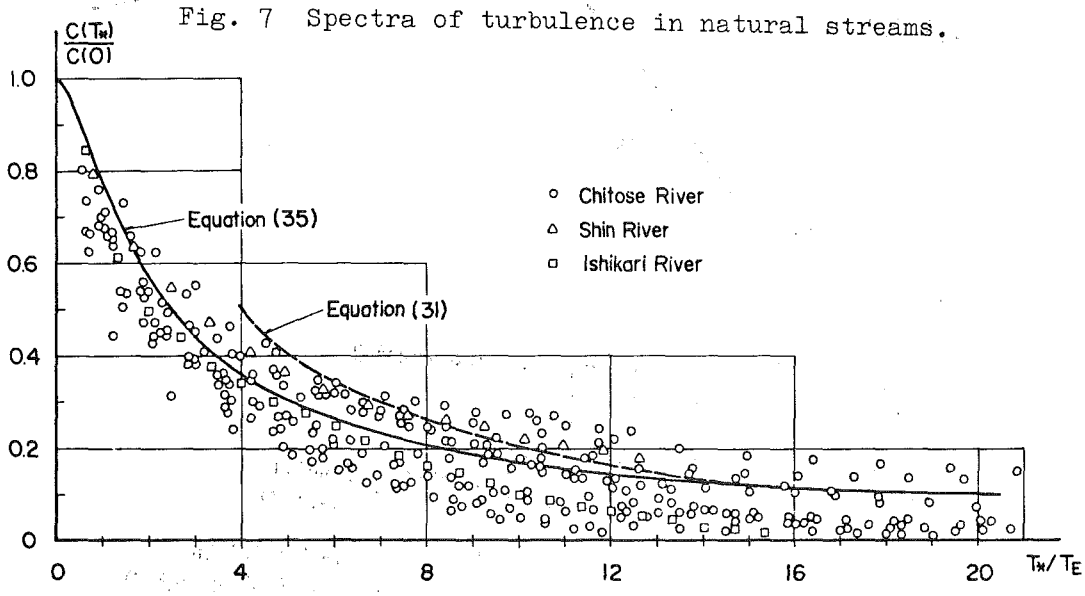

Fig. 8 Variance-duration curve for mean velocity in natural streams.

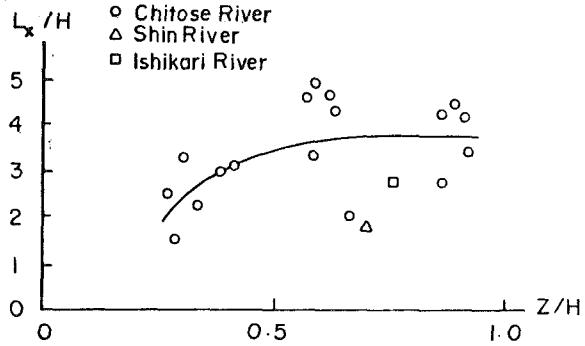

Fig. 9 Relation L_X/H v.s. Z/H.

DISCUSSION

V. T. CHOW

In order to improve the theoretical accuracy of the proposed standard for the observational period, it may be desirable to compute T_E from observed data on velocity fluctuation. Then, there will be a need to propose another standard for the measurement of the velocity fluctuation. It is also important to note that there is an upper constraint for the time of measurement. If the time of observation is too long, the measured data at any point will be greatly affected by the rapid change in velocity due to unsteady nature of the flow particularly at flood stages.

J. W. DELLEUR

Dr. Kishi's paper sheds a new light on the application of linear systems in hydrology.

The classical applications have been the derivation of the kernel function and the output prediction for a given input and kernel. Dr. Kishi addresses himself to the important but less studied problem of the input detection and of the error propagation in such calculations. Little is known about error propagation in hydrologic linear system identification and detection. Laurenson and O'Donnell[1] have studied the error sensitivity of several methods of derivation of the unit hydrograph due to errors of different types in the input and output data. Blank, Delleur, and Giorgini[2] have studied the effect of errors in the kernel function on the output. By means of a perturbation analysis they found that for typical circumstances an error in the kernel is reduced by a factor varying from 1/6 to 1/25 in the calculated output. Conversely, it would appear that an error in the output would be magnified in the derived kernel. This point is now confirmed and amplified in Dr. Kishi's paper which shows that rather small errors in the output data may reduce the precision of identified inputs.

The author then bridges the gap between the sciences of hydrology and turbulence as the latter phenomenon may be the source of errors which propagate in the identification of the hydrologic system input. Mandelbrot and Wallis[3] have suggested that the difference between hydrology and turbulence lies in the the difference in the frequencies of interest, say up to one cycle for the former and above for the latter. Dr. Kishi has now added a new concept of unity between the two sciences often regarded as unrelated.

The results of the measurements of turbulence spectra in natural streams shown in Fig. 7 are of a different order of magnitude from those normally measured in water flows in the laboratory with hot-film anemometers. A recent study by the writer and his associates[4,5] shows that for thin free surface flows, most of the energy is contained at frequencies below 10 cycles per second. Similar conclusions have been obtained by Raichlen[6] and by Richardson and McQuivy[7] for measurements in laboratory flumes. Figure 7 shows that most of the energy is contained in frequencies for which

$$f\,T_E < 0.1 \quad \text{or} \quad f < \frac{0.1}{T_E} \ .$$

If we assume a water depth, H, of 2 meters and a mean velocity, U, of 0.5m/sec, and that the Eulerian time scale is of the order of 5 H/U, then T_E = 20 secs and f = 0.005 cps. This extremely low frequency brings the question as to the

appropriateness of the current meter for turbulence measurement in view of the relatively large time constant of this instrument. Some but few measurements of turbulence with hot film anemometers have been made in rivers and in the ocean.

---

[1]Laurenson, E.M., and O'Donnell, T.: "Data Error Effects in Unit Hydrograph Derivation," Journal of the Hydraulics Division, ASCE, Vol. 95, No. HY6, Nov. 1969.

[2]Blank, D.; Delleur, J.W.; and Giorgini, A.: "Oscillatory Kernel Functions in Linear Hydrologic Models," Paper H58, AGU Annual Meeting (Abstract in EOS, Trans. AGU. Vol. 51, No. 4, April 1970), Submitted for publication in Water Resources Research.

[3]Mandelbrot, B., and Wallis, J.R.: "Noah, Joseph, and Operational Hydrology," Water Resources Research, Vol. 4, No. 5, pp. 909, 1968.

[4]Kisiel, I. T.; Delleur, J. W.; and Rao, Ramachandra A.: "Turbulence Characteristics of Overland Flow," to be presented at the International Association for Hydraulic Research, XIV Congress, Paris, Aug. 29-Sept. 3, 1971.

[5]Kisiel, I. T.: "An Experimental Investigation of the Effect of Rainfall on the Turbulence Characteristics of Shallow Water Flow," Ph.D. Dissertation, School of Civil Engineering, Purdue University, Lafayette, Ind., Jan. 1971.

[6]McQuivery, R. S., and Richardson, E. V.: "Some Turbulence Measurements in Open-Channel Flow," Proc. of the ASCE, Journal of the Hydraulics Division, No. HY1, pp. 209-223, January 1969.

[7]Raichlen, F.: "Some Turbulence Measurements in Water," Proc. of the ASCE, Journal of the Engineering Mechanics Division, No. EM 2, pp. 73-97, April 1967.

P. S. EAGLESON

Would you like to comment upon the practical use of this method in the detection process? Several possible uses come to my mind but of course, all require knowledge of the system function.

a. Filling in missing rainfall records

b. Evaluating the time distribution of rainfall excess

C. KISIEL

1. Can you clarify the procedure used to correct the detected rainfall as shown in Figures 6a and 6b?

2. How representative is the turbulence structure in the river as measured by the current or propeller meter? What effect does this have on the computation of the Eulerian time scale?

3. What would be the effect of sampling errors in precipitation on the extimation of the system frequency function $G(\omega)$? What effect would nonuniformity of rainfall in space (or non-representativeness of the rain gage) have on the entire detection process?

J. PAUL RILEY

In differentiating measured runoff to estimate rainfall input your model does not provide for losses and storage changes within the system. Sometimes these losses are significant in both short time and long time events. You might give consideration to further generalizing your model by taking into account system losses.

V. YEVJEVICH

The author seems to have reached the conclusion that a much longer time measurement of velocities at a point is more important for the accuracy of the computed river discharge than the number of points measured in a river cross-sectional area. From the sampling theory, an optimum must exist between the time of point velocity measurements and the number of points at which velocities are measured. The time-space trade in these measurements that departs from this optimum should result in a loss of accuracy of the computed discharge.

RESPONSE BY T. KISHI

The response to discussion by V.T. Chow is as follows.

The author presented an approximate expression for T_E

$$T_E \simeq (3 \sim 4)H/Um$$

where Um = mean velocity
H = water depth

The value of mean velocity measured in accordance with the present standard, say 60 sec, would be used as a first approximation for Um in the above expression.

However the above expression was derived from the measurements performed in the low water period as stated on page 8 in his paper. And the expression of T_E for the high water has not established.

In this meaning, the author agrees that there is a need to establish a general standard for the measurements of velocity fluctuation.

Response on the discussion by J. W. Delleur and the second question in the discussion by C. Kisiel.

Last year, the author and his colleagues performed the turbulence measurements in open channel flows by the hot film anemometer. The experimental conditions are as follows:

Water depth: 5 ∿ 10 cm ; mean velocity: 40 ∿ 60 cm/sec,
Froude number of flow: 0.5 ∿ 0.8 ; and flows are all
smooth turbulence.

According to our experimental results, the values of the integral time scale T_E were between 0.1 and 0.2 second and most of the turbulence energy were contained at frequencies below 1 ∿ 0.5 cycles per second. This figues of frequency approximately agree with those obtained from $f = 0.1/T_E$ which was pointed out by Prof. Delleur.

As pointed out by Professors Delleur and Kisiel the velocity spectrum measured by the current meter would not be accurate in the high frequency bands, since the current meter is a kind of the cutoff filter for the high frequency bands.

However, the author thinks that the use of the current meter is permissible for the study of the macro structure of turbulence, since the turbulence energy contained in the high frequency bands is relatively small.

The response to discussion by P.S. Eagleson is as follows.

The author performed this calculations aiming at two items pointed out by Prof. P. S. Eagleson. However, it seemed for the author that his aim failed of sucess so far as the examples shown in Figures 6a and 6b are concerned.

The author presumes that one of the reasons of this would be thw too wide Fourier spectrum of the input. Better results in detection process will be expected if a longer sampling interval for the input data is used instead of the hourly rainfall. The author, basing on the precision of the detected input, finds a way of the future development of this method in considering the relationship between the optimum sampling interval of the input and the duration time of the output.

Response to first and third questions in discussion by C. Kisiel.

1) In the calculations shown in Figs.6a and 6b the values of the runoff coefficient are given. The corrected values of the detected rainfall were calculated by dividing the detected rainfall by the runoff coefficient.

3) In the analysis of the runoff systems the Fourier spectra of the inputs are usually far wide than those of the outputs. Consequently, the systems function is liable to be erroneous in the high frequency bands even when the coross-correlation method is used. In this meaning, the author thinks that the use of the high-cut filter such as proposed by Prof. Delleur is necessary.

Response to discussion by J. P. Riley.

In the calculation of the short term runoff, for instant the storm runoff, the definitions of the rainfall loss or the methods of separation of the direct runoff from the total runoff change the funtional form of the outputs and, consequently, have effects on the results of calculations. This effect will be appeared mainly in the low frequency bands of the systems function.

In the calculation of the long term runoff the carry-over discharge to the basin is sometimes a difficult factor to treat as well as the rainfall losses.

The response to discussion by V. Yevjevich is as follows.

As stated by Prof. V. Yevjevich an optimum must exist between the time of point velocity measurements and the number of points at which velocities are measured.

However, in most cases, velocities in a river section vary gradually both in transversal and vertical directions. So that, the increase in the number of points would not improve the precision of the discharge measurements appreciably.

On considering the above fact, the author dared to put stress on the importance of the time of point velocity measurements.